Available online at www.sciencedirect.com
SCIENCE DIRECT®
Journal of the European Ceramic Society 26 (2006) 697–702
www.elsevier.com/locate/jeurceramsoc

# Fabrication of net shape reaction bonded oxide ceramics

H. Geßwein*, J.R. Binder, H.-J. Ritzhaupt-Kleissl, J. Haußelt

*Forschungszentrum Karlsruhe, Institut für Materialforschung III, Postfach 3640, 76021 Karlsruhe, Germany*

Available online 10 August 2005

**Abstract**

Zero-shrinkage mullite-zirconia ceramics with $Y_2O_3$ and MgO as sintering additives and siloxanes as low loss binders were fabricated by direct oxidation of $ZrAl_3/ZrSi_2$ and $ZrAl_3/Zr_2Si/3Y\text{-}ZrO_2$ powder compacts. Depending on the starting composition the sintered ceramics contain either $ZrO_2$ and mullite or $ZrO_2$, alumina and mullite as crystalline phases. The reaction bonding process was studied by thermogravimetry, dilatometry and quantitative XRD-phase analysis. Due to their dense microstructure reaction-bonded 55/45 (vol.%) $ZrO_2$/mullite composites sintered at 1450 °C exhibit biaxial flexure strengths up to 630 MPa. Reaction bonded $ZrO_2/Al_2O_3$/mullite composites (30/25/45 vol.%) show biaxial flexure strengths of 635 MPa.


*Keywords:* Reaction bonding; Composites; Mechanical properties; Mullite; $ZrO_2$

## 1. Introduction

Reaction bonding techniques such as the reaction bonding of aluminum oxide (RBAO) or the reaction bonding of mullite (RBM) are alternative ceramic processing methods offering various advantages over conventional processing routes. Besides their advanced mechanical properties reaction bonded ceramics also exhibit low-to-zero shrinkage during sintering.[1–3] A variant of these reaction bonding techniques is the fabrication of shrinkage-free $ZrSiO_4$-ceramics via the oxidation of the intermetallic compound $ZrSi_2$.[4] One application of this zero-shrinkage ceramic can be found in dentistry where all-ceramic crowns are manufactured.[5]

The process described in this paper is a modified reaction bonding process capable of providing reaction bonded oxide ceramics with high density and zero-shrinkage. Instead of using pure metals intermetallic compounds like $ZrAl_3$, $ZrSi_2$ and $Zr_2Si$ were used as reactive components. During heat treatment in an oxidizing atmosphere the intermetallics oxidize to $ZrO_2$, $Al_2O_3$ and $SiO_2$. The newly formed $Al_2O_3$ reacts with $SiO_2$ to form mullite ($3Al_2O_3{\cdot}2SiO_2$). The oxidation reactions and the mullite formation are associated with a volume expansion which effectively compensates the sintering shrinkage. To improve the compactibility of the starting powder siloxanes are used as so-called low-loss binders. Compared to usually applied binders this type of binder is not totally burnt-out during the pyrolysis but is partially ceramised and so the sintering shrinkage is further reduced. The relative high amount of organic phase in the precursor compacts makes easy green machining possible. So even complex shapes can be formed in the green state and can be reproduced exactly by the reaction bonding process. By adjusting the initial Zr/Al/Si ratio composites belonging to different phase fields in the ternary oxide system $ZrO_2$–$Al_2O_3$–$SiO_2$ can be produced.

The linear length change $\Delta l$ to be expected when a precursor body is converted to a dense reaction bonded ceramic can be estimated from the following equation:

$$\Delta l = \sqrt[3]{\left(1 + \sum_i \tilde{m}_i \Delta\tilde{m}_i\right) \frac{\rho_{gr}}{\rho_s}} - 1 \quad (1)$$

where $\tilde{m}_i$ is the mass fraction of the component $i$, $\Delta\tilde{m}_i$ is the relative mass change of component $i$ and $\rho_{gr,s}$ are the green and sinter densities of the bodies. According to Eq. (1) zero-shrinkage conditions can be achieved by varying the amount

* Corresponding author. Tel.: +49 7247 82 4055; fax: +49 7247 82 4612.
*E-mail address:* holger.gesswein@imf.fzk.de (H. Geßwein).

0955-2219/$ – see front matter © 2005 Elsevier Ltd. All rights reserved.
doi:10.1016/j.jeurceramsoc.2005.06.008

of the mass fractions of the components in the green body which undergo a mass change during reaction forming and adjusting the green density by the compaction pressure. The theoretical sinter density can be calculated if one assumes that the intermetallics oxidize completely and the phase formation follows the thermodynamic stable ternary $ZrO_2$–$Al_2O_3$–$SiO_2$ phase diagram.[6] The relative mass changes can be calculated according to the pyrolysis reaction of the low loss binder and the oxidation reactions of the intermetallics:

$$\Delta\tilde{m}_{\text{siloxane}} = \frac{nM_{SiO_2}}{M_{\text{siloxane}}} - 1 \sim -0,18$$

$$\Delta\tilde{m}_{ZrSi_2} = \frac{M_{ZrO_2} + 2M_{SiO_2}}{M_{ZrSi_2}} - 1 = 0,65$$

$$\Delta\tilde{m}_{Zr_2Si} = \frac{2M_{ZrO_2} + M_{SiO_2}}{M_{Zr_2Si}} - 1 = 0,46$$

$$\Delta\tilde{m}_{ZrAl_3} = \frac{M_{ZrO_2} + (3/2)M_{Al_2O_3}}{M_{ZrAl_3}} - 1 = 0,60$$

where $M_i$ is the molar mass of component $i$ and $n$ is the chain length of the polysiloxane.

Eq. (1) demonstrates that theoretically there are many different compositions resulting in zero-shrinkage ceramics. Practically, however, there exist limitations in the maximum attainable green density of the precursor body depending on the amount of the organic binder. The aim of the present work is to investigate different starting powder compositions which result in the formation of $ZrO_2/Al_2O_3$/mullite and $ZrO_2$/mullite composites. In this paper the fabrication route, phase development and mechanical properties of two selected composites fabricated by this reaction bonding process are described in detail.

## 2. Experimental procedure

The starting powder compositions were calculated in order to obtain 30/25/45 (vol.%) $ZrO_2/Al_2O_3$/mullite and 55/45 (vol.%) $ZrO_2$/mullite composites with zero-shrinkage after the reaction bonding process. The amount of $Y_2O_3$ was chosen such that a $ZrO_2/Y_2O_3$ molar ratio of 97/3 in the final ceramic was obtained. Table 1 lists the powder compositions AZM1 and ZM1.

Table 1
Starting compositions of the reaction bonded ceramics

| Sample | Weight fraction (wt.%) | | | | | | |
|---|---|---|---|---|---|---|---|
| | $ZrAl_3$ | $ZrSi_2$ | $Zr_2Si$ | $ZrO_2$[a] | $Y_2O_3$[b] | MgO[c] | Siloxane |
| ZM1 | 43.78 | – | 34.21 | 10.38 | 4.69 | 1.00 | 5.94 |
| AZM1 | 78.74 | 11.02 | – | – | 3.79 | 0.49 | 5.95 |

[a] Tosoh-Zirconia TZ-3Y.
[b] Alfa Aesar REacton 99.99%.
[c] Merck.

To manufacture the ceramics $ZrSi_2$ and $Zr_2Si$ (H.C. Starck 99%) were ball-milled for 48 h in 2-propanol. $ZrAl_3$ (Alfa Aesar 99%) was cryo-milled for 0.25 h in liquid nitrogen (SPEX CertiPrep Freezer/Mill 6800). After cryo-milling the aluminide was passed through a 125 μm sieve. Then the starting powder mixtures were homogenized for 24 h in a planetary ball mill with $ZrO_2$ milling balls in 2-propanol. The amount of $ZrO_2$ milling debris revealed by gravimetry was <0.2 wt.%. The siloxane (Wacker Silres K) was added at the end of the milling process. The suspensions were converted into granules by spray-drying, which were densified afterwards by uniaxial pressing. The compaction pressure to achieve the necessary green density for zero-shrinkage, in both cases 75% of the theoretical green density, was determined through compaction curves as shown in Fig. 1. Densities of the green bodies were calculated from weight and geometry of the cylindrical specimens. The green compacts were fired in box furnaces in flowing air using the following typical heating cycle: 5 °C/min → 300 °C, 0.3 °C/min → 900 °C, 2 h hold, 10 °C/min → 1450 °C (1500 °C), 1 h (3 h) hold, 10 °C/min → room temperature. Disc samples (diameter of 15 mm) for strength measurements were machined to a height of 1.2 mm and finally polished down to a 20–25 μm finish by using a SiC suspension.

Changes of weight and dimension which occurred during the reaction sintering were monitored by thermogravimetry (Netzsch STA 449C) and dilatometry (Netzsch DIL 402C). Final sintered densities were measured by the Archimedes method, and the microstructures of polished surfaces were investigated via scanning electron microscopy (Jeol JSM 6400). Phase analysis was carried out by X-ray powder diffractometry (XRD) in step scan mode using Cu Kα radiation (Siemens D5005). Phase compositions of the reaction bonded samples were quantitatively determined by the Rietveld method using the software package GSAS.[7] Strengths were measured according to DIN EN ISO 6872 by punch on three equally spaced ball loading, using a punch 1.1 mm in diameter with the balls lying on a circle 12 mm in diame-

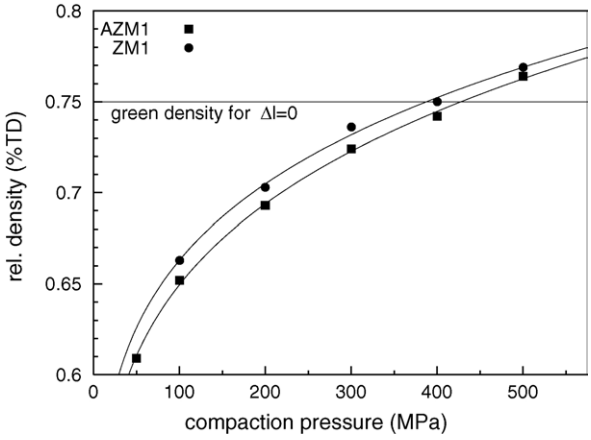


Fig. 1. Relative density dependence on uniaxial compaction of granules AZM1 and ZM1.

ter. The Weibull parameters were estimated by the traditional least-squares method on the basis of a relatively small sample size of 12 specimens. Vicker's hardness were determined by a hardness tester (Leco V-100-C1).

## 3. Results and discussion

### 3.1. Reaction bonding process

Simultaneous thermal analysis and dilatometry were used to investigate the processes occurring during reaction bonding. These processes can be summarized as follows: (a) pyrolysis of the Si-polymer into $SiO_2$, (b) oxidation of the intermetallic compounds to the corresponding oxides, (c) phase formation and (d) sintering. Fig. 2 shows the TG–DSC curves of sample AZM1. The broad exothermic peak at 760 °C is attributed to the oxidation reactions of $ZrAl_3$ and $ZrSi_2$. The shoulder on the left side of this peak clearly indicates two overlapping exothermic processes. At about 900 °C there is no further weight gain and the oxidation of the intermetallics is nearly completed. The minor exothermic peak at 960 °C is connected with the crystallisation of the newly formed amorphous $Al_2O_3$ to metastable transition alumina. The TG–DSC curves show that the oxidation step of the reaction-bonding process is critical because the strong heat release during the exothermic oxidation can lead to local overheating of samples. This has to be taken into account when planning heating schedules for larger samples. The weight and dimensional changes of samples ZM1 and AZM1 during typical thermal treatments are given in Fig. 3. In both cases green bodies begin to expand at temperatures about 450 °C. From the thermal hold at 900 °C onwards there is no more weight and length gain. After the hold the sintering process starts and the bodies begin to shrink. The sintering is completed after the final thermal hold at 1450 °C for ZM1 and 1500 °C for AZM1. As can be seen from the small peak in the dilatometer output in Fig. 3 (material AZM1), formation of mullite from $Al_2O_3$ and $SiO_2$, which is associated with a volume expansion of ~4%, occurs at 1280 °C and is essentially completed at 1380 °C, whereupon densification continues. At the end the reaction bonded composites are white-coloured and exhibit approximately zero linear shrinkage.

### 3.2. Phase development

The room-temperature XRD spectra of green bodies and of as-fired surfaces of materials ZM1 and AZM1 after heating to temperatures of 900 to −1200 °C are shown in Fig. 4(a) and (b), respectively. These spectra enable us to monitor the phase changes occurring during the reaction forming. The XRD pattern of the green body of material ZM1 shows the peaks of $ZrAl_3$, $Zr_2Si$, $ZrO_2$ and $Y_2O_3$ as expected. The spectra of the sample heated to 900 °C consists mainly of broad peaks of t-$ZrO_2$ and m-$ZrO_2$. At that temperature there has been no reaction between $Y_2O_3$ and the newly formed

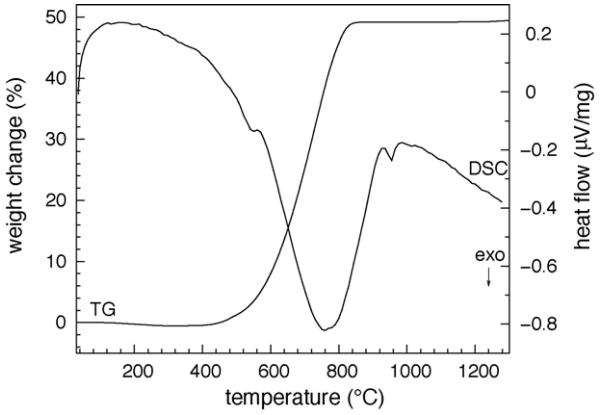


Fig. 2. TG–DSC curves recorded during heating of AZM1 granules (sample mass ~30 mg) up to 1300 °C at a rate of 10 °C/min in flowing air.

$ZrO_2$. The crystallographic form of $Al_2O_3$ is not evident from this spectra because the metastable transition aluminas show weak diffraction peaks[8] overlapping with the peaks of the zirconia phases. Mullitization and the crystallisation of α-$Al_2O_3$ begins at a temperature of 1100 °C, as can be seen from the $(1\,0\,\bar{2})$ α-$Al_2O_3$ peak at $2\theta = 25.65°$ and the very

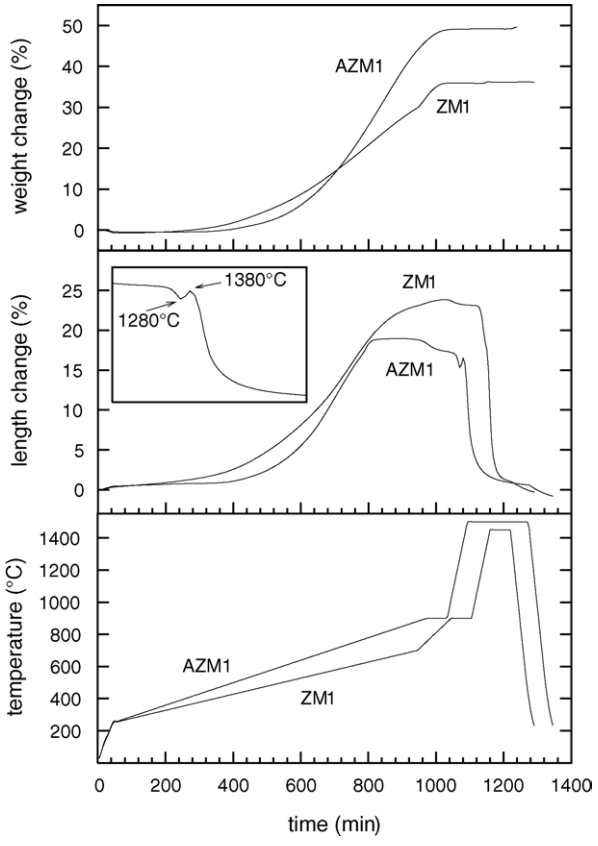


Fig. 3. Weight and dimensional changes of materials AZM1 and ZM1 compacted at 430 and 400 MPa, respectively (specimens: green bodies with Ø = 5.9 mm). The two different heating cycles are also included. An expanded region of dilatometer curve of sample AZM1 is shown in the inset of the figure to show mullite formation.

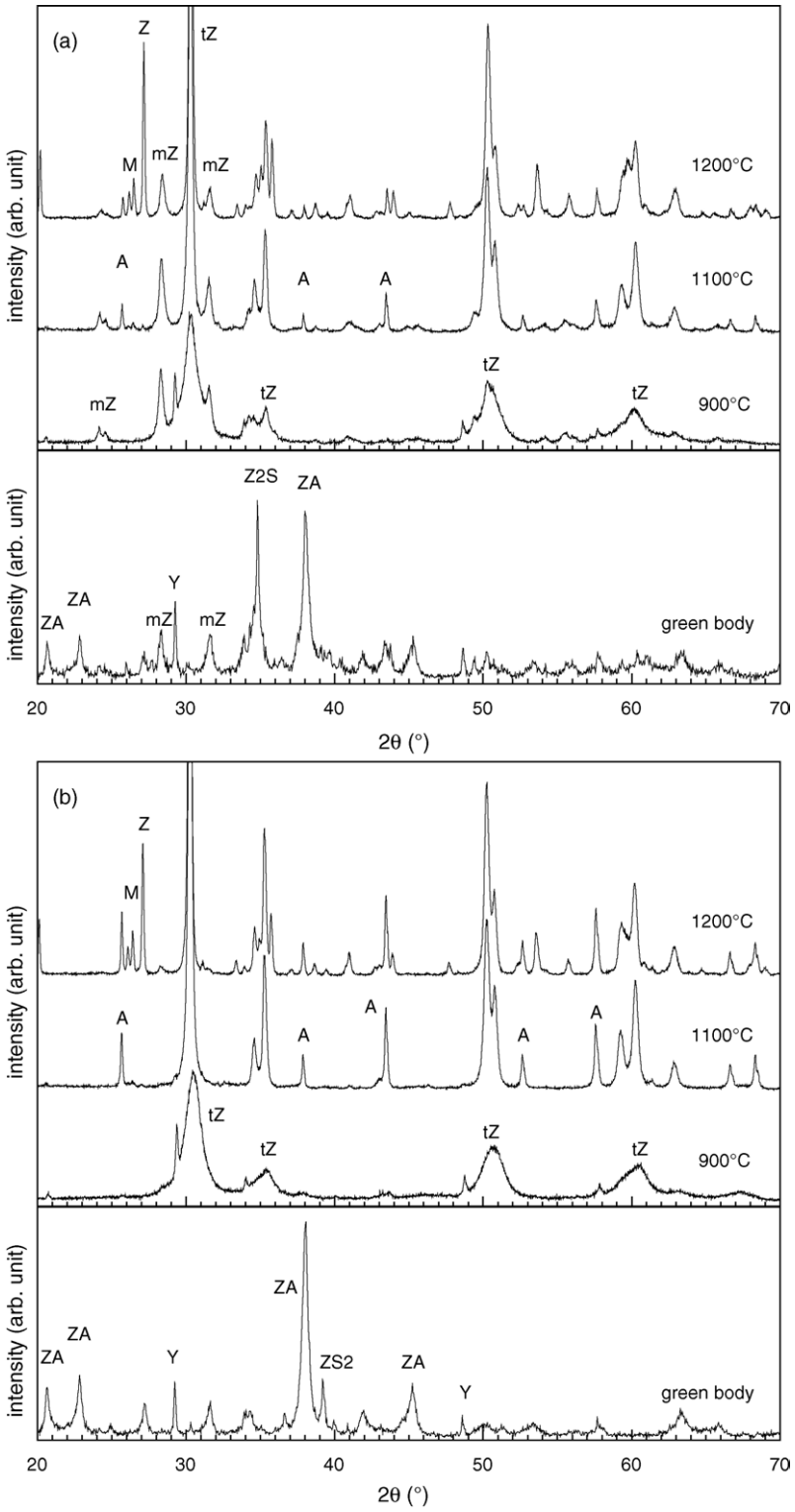


Fig. 4. XRD patterns showing the phase development during reaction bonding ((a) ZM1 and (b) AZM1). The samples were heated to the appropriate temperature, held for 2 h, and then cooled. ZA = $ZrAl_3$, ZS2 = $ZrSi_2$, Z2S = $Zr_2Si$, Z = zircon, M = mullite, tZ = t-$ZrO_2$, mZ = m-$ZrO_2$, A = $Al_2O_3$.

weak (2 1 0) mullite peak at $2\theta = 26.35^\circ$. This peak is clearly visible at 1200 °C. In concurrence to the mullite formation the reaction of $ZrO_2$ with amorphous $SiO_2$ to zircon takes place. Zircon is a transient phase and disappears at temperatures of 1400 °C. The formation of Zircon as an intermediate phase in the $ZrO_2$/mullite system has been reported previously.[9,10] The XRD patterns of the samples heated to 1400–1550 °C show that the main phases are mullite, m- and t-$ZrO_2$ with a

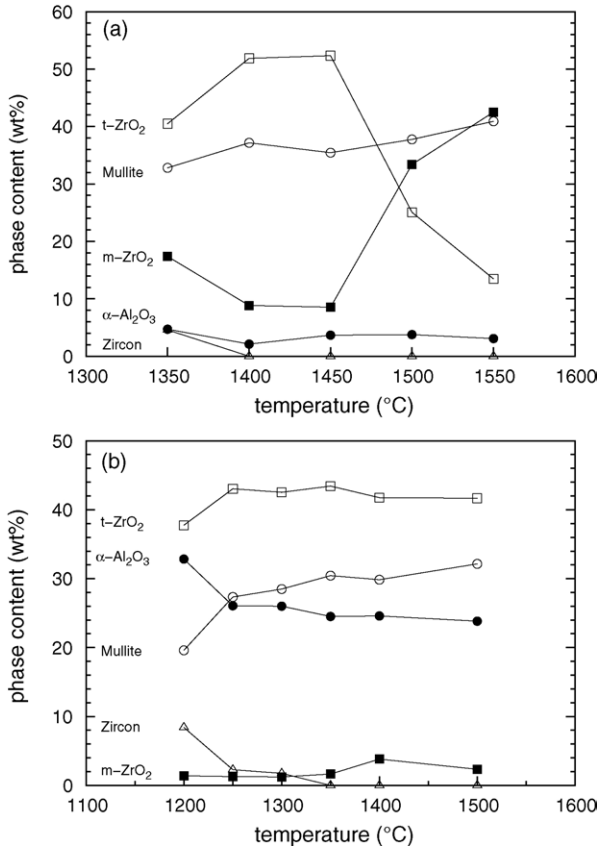


Fig. 5. Variation of quantitative phase compositions during different heat treatments obtained from Rietveld analysis ((a) ZM1 and (b) AZM1).

trace of α-$Al_2O_3$ still present in these material. For material AZM1 the XRD patterns reveal the same phase formation sequence as in material ZM1. The pattern of the sample heated at 1100 °C indicates the first formation of zircon and mullite with the appearance of very weak diffraction peaks of these two phases. At 1200 °C these peaks have much higher intensity. In this material zircon already disappears at temperatures of 1350 °C. The fully reaction bonded composite consists of mullite, alumina, m- and t-$ZrO_2$. To get a quantitative estimate of the relative proportions of the various phases present, especially the ratio of tetragonal to monoclinic zirconia, the spectra were analysed with the Rietveld method. In Fig. 5 the variation of quantitative phase composition with the sintering temperature obtained from the Rietveld analysis for the two materials are presented. The estimated errors in the determined weight fractions are in the range of ± (1–3)%. At 1450 °C the reaction bonded composite ZM1 contains 52.3 wt.% t-$ZrO_2$, 8.6 wt.% m-$ZrO_2$, 35.5 wt.% mullite and 3.7 wt.% α-$Al_2O_3$. With increasing sintering temperature the amount of m-$ZrO_2$ in the ceramic steadily increases. As can be seen from Fig. 5(b) the phase content of sample AZM1 does not change significantly above temperatures of 1350 °C. The sample sintered at 1500 °C finally consists of 41.7 wt.% t-$ZrO_2$, 2.3 wt.% m-$ZrO_2$, 32.1 wt.% mullite and 23.8 wt.% α-$Al_2O_3$.

From the XRD results and thermal analysis the phase formation processes during the thermal treatment of materials ZM1 and AZM1 can be summarized as follows:

$T < 600\,^{\circ}C$: $[Si(CH_3)O_{1,5}]_n \xrightarrow{air} SiO_2 + \cdots$

$T > 450\,^{\circ}C$: $ZrAl_3 \xrightarrow{air} ZrO_2 + \frac{3}{2}Al_2O_3$

$Zr_2Si \xrightarrow{air} 2ZrO_2 + SiO_2$

$ZrSi_2 \xrightarrow{air} ZrO_2 + 2SiO_2$

$T > 1100\,^{\circ}C$: $ZrO_2 + SiO_2 \rightleftarrows ZrSiO_4$

$3Al_2O_3 + 2SiO_2 \rightleftarrows 3Al_2O_3{\cdot}2SiO_2$

$T > 1300\,^{\circ}C$: $2ZrSiO_4 + 3Al_2O_3 \rightleftarrows 2ZrO_2 + 3Al_2O_3{\cdot}2SiO_2$

### 3.3. Microstructure

The microstructures of samples AZM1 and ZM1 are shown in Fig. 6(a) and (b), respectively. The $ZrO_2$ phases appear brighter due to atomic number contrast in comparison with Al- and Si-containing alumina and mullite phases which appear gray. Examination of Fig. 6 reveals that the $ZrO_2$ particles exhibit equiaxed grains with sizes <1 μm. Some of the $ZrO_2$ grains are distributed inside the alumina or mullite grains. As it is evident from the SEM micrograph of sample ZM1 the mullite particles show an elongated morphology with relatively large sizes of about 2–3 μm. In addition, the

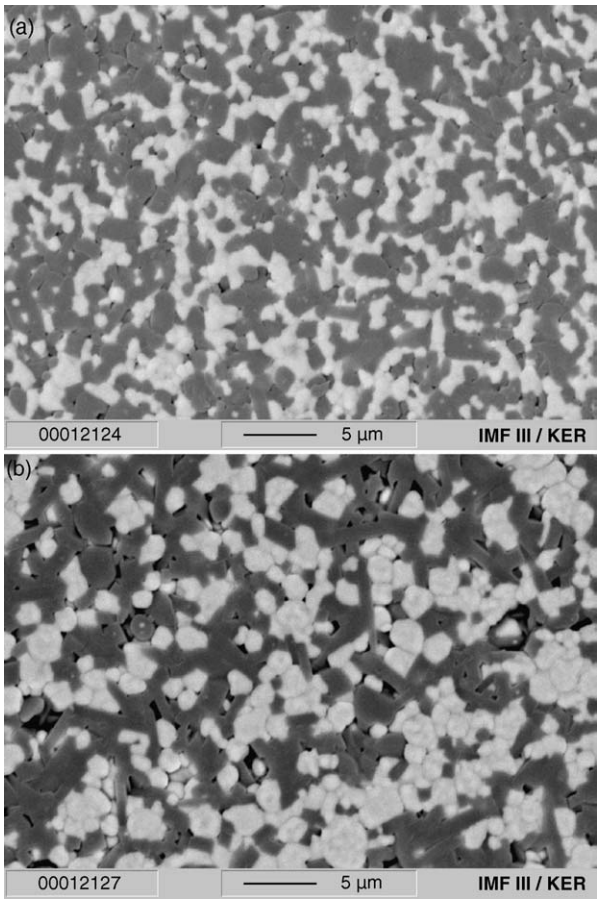


Fig. 6. SEM micrographs showing the microstructures of reaction bonded $ZrO_2/Al_2O_3$/mullite (a) and $ZrO_2$/mullite composites (b).

Table 2
Physical and mechanical properties of the ceramics

| Material | $\rho_{sinter}$ (g/cm$^3$) | $\rho_{sinter}$ (% TD) | $\sigma_0$ (MPa)[a] | m | H (HV10) |
|---|---|---|---|---|---|
| AZM1 | 4.21 | 98.8 | 635 | 18 | 1250 |
| ZM1 | 4.31 | 96.6 | 632 | 12 | 1190 |

[a] Biaxial flexure strength.

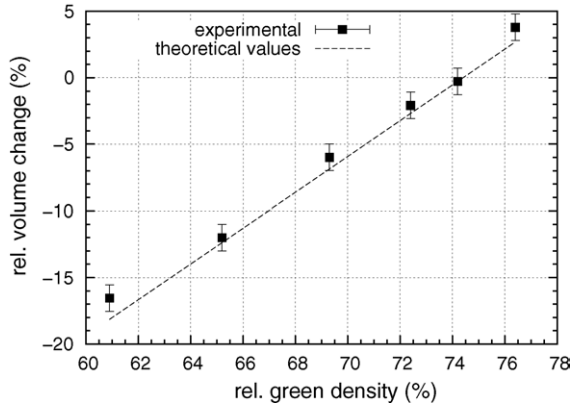


Fig. 7. Relative volume change as a function of green density for material AZM1.

sample contains some pores. Both composites show a fairly dense microstructure with bulk densities of about 97–98% of the theoretical density, which was calculated using the theoretical densities of the individual phases and the composition determined by Rietveld analysis.

### *3.4. Mechanical properties and sinter shrinkage*

The biaxial flexural strength and Vickers hardness of the AZM1 and ZM1 specimens are listed in Table 2. The estimated parameters of AZM1 and ZM1 are $\sigma_0 = 635$ MPa, $m = 18$ and $\sigma_0 = 632$ MPa, $m = 12$, respectively. Vickers hardness of the two ceramics are 1250 HV10 for AZM1 and 1190 HV10 for ZM1. These strength values are comparable with those of conventional mullite and reaction bonded mullite ceramics.[11]

To examine the sinter shrinkage in more detail and to verify the theoretical volume changes predicted by Eq. (1) samples of material AZM1 were compacted at different uniaxial pressures to achieve different green densities. Fig. 7 reveals how the volume change during the reaction bonding process depends on the green density. The straight line in the figure represents the theoretical volume change as a function of green density and the symbols are the experimentally determined volume changes. For the calculation of the theoretical volume changes the relative mass changes were determined experimentally. These values and the weight fractions according to composition AZM1 were used as fixed parameters. The sinter density was assumed to be 98% of the theoretical density. This was confirmed by density measurements of the samples sintered at 1500 °C for 3 h. As can be seen from Fig. 7 the theoretical and experimental data are in good agreement within the margin of experimental error.

## 4. Conclusions

Dense and shrinkage-free $ZrO_2/Al_2O_3$/mullite and $ZrO_2$/mullite composites were produced by a reaction bonding process using a combination of $ZrAl_3/ZrSi_2$ and $ZrAl_3/Zr_2Si$ as reactive precursor materials. To increase the compressibility of the starting powders a low loss binder was used. The sinter shrinkage can be effectively compensated by the volume increase associated with the oxidation of the intermetallics and the phase formation of mullite. During reaction forming zircon is formed as an intermediate phase and disappears at temperatures above 1300 °C. The composites can be sintered to high density at temperatures of 1450–1500 °C. Due to their fine grained microstructure they exhibit biaxial flexure strengths up to 635 MPa.

## References

1. Claussen, N., Le, T. and Wu, S., Low-shrinkage reaction-bonded alumina. *J. Eur. Ceram. Soc.*, 1989, **5**, 29–35.
2. Holz, D., Pagel, S., Bowen, C., Wu, S. and Claussen, N., Fabrication of low-to-zero shrinkage reaction-bonded mullite composites. *J. Eur. Ceram. Soc.*, 1996, **16**, 255–260.
3. She, J. H., Schneider, H., Inoue, T., Suzuki, M., Sodeoka, S. and Ueno, K, Fabrication of low-shrinkage reaction-bonded alumina–mullite composites. *Mater. Chem. Phys.*, 2001, **68**, 105–109.
4. Hennige, V. D., Haußelt, J., Ritzhaupt-Kleissl, H.-J. and Windmann, T., Shrinkage-free $ZrSiO_4$-ceramics: characterisation and applications, *J. Eur. Ceram. Soc.*, 1999, **19**, 2901–2908.
5. Binder, J. R., Ritzhaupt-Kleissl, H.-J. and Haußelt, J., *Keramischer Zahnersatz aus einer schwindungsfreien Zirkonkeramik*. dental dialogue, 2. Jahrgang 6, 2001.
6. Ondik, H. M. and McMurdie, H. F., ed., *Phase Diagrams for Zirconium + Zirconia Systems*. The American Ceramic Society, 1998.
7. Larson, A. C. and Von Dreele, R. B., *General Structure Analysis System (GSAS)*. Los Alamos National Laboratory Report LAUR 86–748, 2000.
8. Lippens, B. C. and de Boer, J. H., Study of phase transformations during calcination of aluminum hydroxides by selected area electron diffraction. *Acta Crystallographica*, 1964, **17**, 1312–1321.
9. Di Rupo, E. and Anseau, M. R., Solid state reactions in the $ZrO_2{\cdot}SiO_2$–$\alpha$-$Al_2O_3$ system. *J. Mater. Sci.*, 1980, **15**, 114–18.
10. Scheppokat, S., Janssen, R. and Claussen, N., Phase development and shrinkage of reaction-bonded mullite composites with silicon carbide of different particle sizes. *J. Am. Ceram. Soc.*, 1999, **82**, 319–324.
11. Wu, S., Chan, H. M. and Harmer, M.P., Reaction-forming of mullite ceramics using an aqueous milling medium. *J. Am. Ceram. Soc.*, 1997, **80**, 1579–1582.